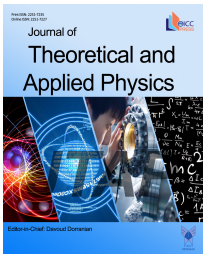

Volume 18, Issue 5, 182459 (1-9)

Journal of Theoretical and Applied Physics (JTAP)

https://dx.doi.org/10.57647/j.jtap.2024.1805.59

Spin filtering device through designing the normal/ferromagnetic/normal graphene superlattices

Saeedeh Mohammadi[1], Ayoub Esmailpour[1,*], Mehdi Saadat[1], Hamed Meshkin[2]

[1]*Department of Physics, Shahid Rajaee Teacher Training University, Tehran, Iran.*
[2]*Department of Physics, Purdue University, Indianapolis, Indiana, USA.*

[*]**Corresponding author:** esmailpour@sru.ac.ir

Original Research

Received:
23 June 2024
Revised:
11 August 2024
Accepted:
23 August 2024
Published online:
30 October 2024

Abstract:

Quantum transport properties of normal/ferromagnetic/normal graphene (NG/FG/NG) superlattices exposed to ferromagnetic graphene connected to a gate electrode are investigated via the transfer matrix method. Here, we calculate the role of parameters including well, and barrier width in the spin current. In addition, the Fermi energy and gate voltage effects on raising and tunable spin splitting have been investigated. Calculations demonstrate that the exchange field applied to the region of the ferromagnetic graphene device, by changing the chemical potential, results in an oscillatory behavior. We found that it opens a gap and indicates a metal-insulator phase transition by enhancing unit cells (N = 100). Meanwhile, results reveal that by tuning the gate voltage, we can control the spin currents, as a result, it may allow for the filtering of up or down spins. Further, increasing the barrier width and Fermi energy reveals that the spin current is reversible. Furthermore, this computational research found that quantum modulating behavior by controlling wells, barrier widths, and chemical energy in the device. The results might have potential applications in designing nano-devices and developing spintronic systems.

Keywords: Graphene superlattice; Transfer matrix; Spin filtering; Spintronic

1. Introduction

Spintronics in ultrathin two-dimensional (2D) materials, e.g., graphene and graphene-like, recently attracted a lot of attention [1–3]. The spin degree of freedom of electrons in these materials could be useful in designing high-efficiency spin logic devices [4–6]. Besides, the electronic properties of graphene monolayers [7–10] and bilayers [11] in low-energy concepts have been a subject of great interest for decades. Graphene has an electron mobility of at least 10000 cm^2/Vs which ten times higher than the electron mobility of silicon wafers used in microprocessors [12]. The energy bands in the honeycomb lattice, i.e., graphene, and silicene, are described by the two-dimensional Dirac's equation, and in this regard, the hexagonal corners are known as Dirac's points for the Brillouin zone.

It is known that the electron conductance of a graphene-based superlattice significantly relates to the structural parameters of the superlattice [13, 14]. In recent years, the graphene-based junctions, i.e., superconductor, ferromagnetic (FM), and insulator, have been the focus of intense research due to their application in spintronic devices [15–18]. Spin-polarized current via injunction into metallic systems [19], semiconductors [20], and graphene [21] was investigated by several research groups. Due to the proximity effect in the graphene-based FM, the spin-down and spin-up electrons are separated from each other, so, the spin current is polarized. As a result, the spin-polarized carriers are the key for spintronic applications. By adding a magnetic layer in the graphene-based junction, we can intensify the effect of magnetic tunnel junction (MTJ) [22]. Yuasa et al. [23] revealed that in the ferromagnetic/insulator/nonmagnetic/-ferromagnetic (FM/I/NM/FM) junction, the tunnel magnetoresistance (TMR) has an oscillatory behavior, which is linked with the thickness of the non-magnetic (NM) layer. Also, Mu et al. [24] and Yang et al. [25] showed that this oscillatory behavior was an intrinsic feature of the junctions.

Lu [26] observed that the spin-polarization is enhanced by increasing the gate voltage with a double magnetic barrier. Increasing the bias field causes the spin-dependence of the quantum modulation on the separation between the two magnetic fields to become more regular in the junction [27, 28].

Graphene junction structures such as ferromagnetic/insulator/ferromagnetic (FM/I/FM) [29], ferromagnetic/normal/-ferromagnetic (FM/N/FM) [30], and ferromagnetic/insulator/ d(p)-wave superconducting (FM/I/ d(p)-wave S) [31] were evaluated broadly in recent studies. The spin transport is observed in a graphene-based MTJ. Besides, by applying a magnetic field, the spin conductance reveals an oscillatory behavior in the ferromagnetic graphene (FMG) superlattice which, this behavior indicates as spin filtering [32]. In suspended graphene-based spin-valve devices [33], graphene sits a few hundred nm above the substrate, and therefore spin transport will not be affected by impurity scattering from the substrate. For sure, these devices will answer the question, of how is spin information lost in graphene apart from the Elliot-Yafet mechanism. Pi et al. experimentally focused on the spin injection process in graphene using a Co element with TiO_2 seeded MgO barriers. Their experiments, conducted at room temperature, demonstrated that tunnel barriers reduce spin relaxation caused by contact and are crucial for studying spin relaxation in graphene [34]. In a different experimental approach, researchers in China found that the generation of highly spin-polarized current could be controlled by adjusting the transverse electric field, source temperature, and the width of a graphene nanoribbon (GNR) device [35]. Zigzag graphene nanoribbons (ZGNRs) are emerging as a new type of magnetic nanomaterial, potentially serving as building blocks for thermally driven spin circuits. However, from a device preparation point of view, it is challenging to make FM contacts on the suspended graphene and perform spin transport measurements. We have previously reported the structures of disordered, i.e., strain-induced [36], graphene [37, 38], and graphene-like [39] superlattices for the design of electronic nano-devices. Niu et al. [40] explored the magnetic proximity effect and local exchange splittings in normal/ferromagnetic/normal/-ferromagnetic.../normal graphene superlattices, finding that gate voltage can enhance spin polarization and the magnetoresistance (MR) ratio. Bezerra and Lima [41] focused on how transport sensing relates to the modulation of the Fermi velocity, revealing an angle-dependent miniband and mini-gap structure in transmission magnetic graphene superlattice. Lima et al. [42] studied the effect of Fermi velocity on electronic transmission, noting that tuning the Fermi velocity affects total conductance and the Fano factor. Despite these advancements, challenges remain in fabricating these devices. The tuning of well and barrier widths is crucial for developing efficient nano-devices. Based on the findings, we believe that adjusting parameters such as well width, barrier width, Fermi energy, and exchange field in the FG superlattice could lead to significant applications in the nano-electronics industry. Meanwhile, the behaviors mentioned about FMG may be intensified in the superlattice structure of FMG. Although, there are some reports of graphene junction structures, the normal/ferromagnetic/normal graphene (NG/FMG/NG) superlattices as a spin filter deserve more attention. This behavior, modulated by the gate voltage, suggests potential applications in spintronics, particularly for tunable spin current and spin filtering systems.

In the present paper, we investigated the spin transport of NG/FMG/NG superlattices in which a gate electrode is connected to the FMG. We revealed that the spin current through the superlattice has an oscillatory behavior. This oscillatory behavior is generated due to the exchange field of the FMG. This behavior depends on the chemical potential of the FMG, which is tunable by the gate voltage. Therefore, our system can play as a tunable spin current and spin-filtering. Also, it can be useful for the development of spintronic systems.

2. Model and method

Details of the formulation and numerical calculation of the method are as follows. In graphene, the fermions in the Fermi level are described by a massless Dirac equation. Figure 1 (a) represents a two-dimensional NG/FMG/NG/... superlattice when a gate electrode is connected to the FMG. Applying a transverse electric field on the graphene nanoribbon (GNR) causes the superlattice partially to be capable of behaving as ferromagnetic. The schematic model of the dispersion relations is shown in Figure 1 (b). The ith interface labeles by L_i where, $L_i = \text{int}[i/2]\, D + \text{int}[(i-1)/2]\, L$. Meanwhile, there is a valley degeneracy, we focused on the Hamiltonian H_+ with

$$H_+ = v_F(\sigma_x k_x \pm \sigma_y k_y) - V(x), \tag{1}$$

where

$$V(x) = \begin{cases} E_F & : \text{NG} \\ E_F + U + \eta_{\uparrow\downarrow} h & : \text{FG} \end{cases} \tag{2}$$

where σ_x and σ_y are Pauli's matrices, $v_F \approx 10^6$ (m/s) as fermi velocity and η denotes for up and down spins. Also, $E_F = v_F k_F$ is the fermi energy, U is the chemical potential shift, and h is the exchange field.

The incident of the massless electron in the superlattice propagates at an angle φ along the x-axis. Therefore, the wave functions, which are described by the Dirac Hamiltonian, the following equations:

$$\Psi_1 = \begin{pmatrix} 1 \\ e^{i\varphi_i} \end{pmatrix} e^{ik_{(i-1)x}\cos\varphi_i x + ik_y y} + a_i \begin{pmatrix} 1 \\ -e^{-i\varphi_i} \end{pmatrix} e^{-ik_{(i-1)x}\cos\varphi_i x + ik_y y} \tag{3}$$

$$\Psi_2 = b_i \begin{pmatrix} 1 \\ e^{i\varphi_i} \end{pmatrix} e^{ik_{i\pm x}\cos\varphi_i x + ik_y y} + c_i \begin{pmatrix} 1 \\ -e^{-i\varphi_i} \end{pmatrix} e^{-ik_{i\pm x}\cos\varphi_i x + ik_y y} \tag{4}$$

$$\Psi_3 = d_i \begin{pmatrix} 1 \\ e^{i\varphi_i} \end{pmatrix} e^{ik_{(i+1)x}\cos\varphi_i x + ik_y y} \tag{5}$$

Here, Ψ_1 and Ψ_3 are the wave functions for regions left and right, respectively. In this relations $p = k$ and

$$k_i = \begin{cases} k_{i+1} = \frac{E_F}{V_F} = k_{i-1} & : \text{NG} \\ k_i = \frac{E_F + U \pm h}{V_F} & : \text{FG} \end{cases} \tag{6}$$

$$\varphi_i = \begin{cases} \varphi & \text{for well} \\ \theta & \text{for barrier} \end{cases} \tag{7}$$

To calculate the transmission coefficients of superlattice, we used the transfer-matrix method [13]. Therefore, we applied the continuity of the wave function at the boundaries and constructed the transfer matrices as follows:

$$\begin{pmatrix} 1 \\ r \end{pmatrix} = \frac{1}{\cos(\varphi_i)} M S(x) N t_{2N} \tag{8}$$

here t_{2N} and r are the transmission and reflection coefficients, respectively, for N magnetic barriers in the system.

$$M = \begin{pmatrix} e^{-i\varphi} - e^{i\theta} & e^{-i\varphi} + e^{-i\theta} \\ e^{i\varphi} + e^{i\theta} & e^{i\varphi} - e^{-i\theta} \end{pmatrix}, \tag{9}$$

$$N = \begin{pmatrix} e^{ik_x L_N}(e^{-i\theta} - e^{i\varphi})/2e^{ik_{\pm x} L_N} \cos\theta \\ e^{ik_x L_N}(e^{i\theta} + e^{i\varphi})/2e^{-ik_{\pm x} L_N} \cos\theta \end{pmatrix}, \tag{10}$$

$$S(x = L_i) = \begin{pmatrix} t_{11} & t_{12} \\ t_{21} & t_{22} \end{pmatrix}, \quad \mathrm{S(x)} = \mathrm{S}(L_2), \mathrm{S}(L_3) \ldots \mathrm{S}(L_{N-1}), \tag{11}$$

where

$$\begin{aligned} t_{11} &= e^{i(k_{(i\pm)x} - k_{(i-1)x})L_{i-1}} \left[e^{i\varphi_i} + e^{-i\varphi_{i-1}}\right] \Big/ 2\cos(\varphi_{i-1}) \\ t_{12} &= e^{i(-k_{(i\pm)x} - k_{(i-1)x})L_{i-1}} \left[-e^{-i\varphi_i} + e^{-i\varphi_{i-1}}\right] \Big/ 2\cos(\varphi_{i-1}) \\ t_{21} &= e^{i(k_{(i\pm)x} + k_{(i-1)x})L_{i-1}} \left[-e^{i\varphi_i} + e^{i\varphi_{i-1}}\right] \Big/ 2\cos(\varphi_{i-1}) \\ t_{22} &= e^{i(-k_{(i\pm)x} + k_{(i-1)x})L_{i-1}} \left[e^{-i\varphi_i} + e^{-i\varphi_{i-1}}\right] \Big/ 2\cos(\varphi_{i-1}) \end{aligned} \tag{12}$$

It is evident that $T(E_0, \varphi) = |t_{2N}|^2$ and that it can be calculated from the above equations by a given N. Now, by using transmission coefficients are calculated, the electron conductance is described by the Buttiker formula [43] is given by

$$G = G_0 \int_{-\pi/2}^{\pi/2} T(E, \varphi) \cos\varphi \, d\varphi, \tag{13}$$

where $G_0 = e^2 mvw/\hbar^2$ with w is the width of the graphene in the y direction. And finally, we computed the spin conductance for $G_{\uparrow\downarrow} = \frac{1}{2} \int_{-\pi/2}^{\pi/2} T_{\uparrow\downarrow}(\varphi) \cos\varphi \, d\varphi$ by means of

$$G_S = G_\uparrow - G_\downarrow. \tag{14}$$

3. Numerical results and discussion

Using Eq. (14), we calculated the conductance to study the transport properties of the FMG superlattice. The conductance of spin-up and down as a function of chemical

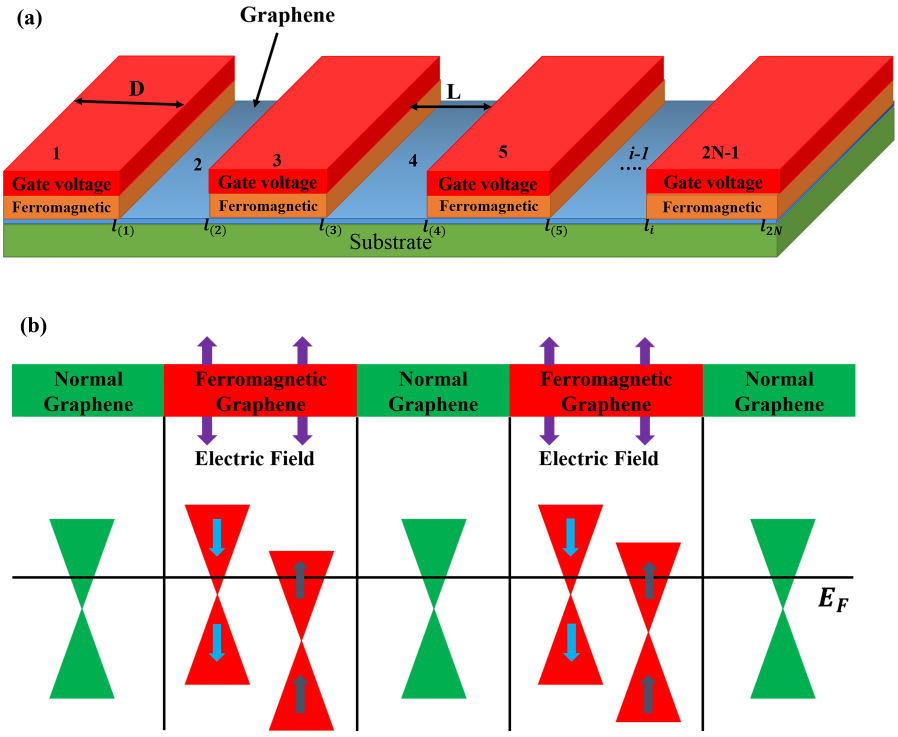

Figure 1. The model of a normal/ferromagnetic/normal graphene (NG/FMG/NG) superlattice junctions. (a) Schematic illustration of NG/FMG/NG superlattice with ferromagnetic layer and gate voltage (b) model of NG/FMG/NG superlattice junctions with corresponding Dirac cones.

potentials (U) in the superlattice is illustrated in Figure 2. The spin-dependence of the charge carrier's conductance through the FMG superlattice with the different number of barriers was evaluated in our study. All the initial values in Figure 2 are as follows: the Fermi energy of the incident electron $E_F = 300$ (meV), exchange field $h = 10$ (meV), barrier width $D = 42.5$ (nm), and well width $L = 4.5$ (nm). In this regard, Figure 2 (a) shows an FMG superlattice with the number of magnetic barriers as, $N = 100$. Since, we would like to observe the π-periodicity, we have focused on the range of $|U \pm h| \gg E_F$. It can be seen that the conductance has $\pi-$periodicity behavior depents to UL/v_F or $UL/v_F \pm HL/v_F$ [28]. Meanwhile, the maximum (minimum) value of conductance is equal to 0.7 (almost zero). The difference between up and down spin is equal to $2hL/v_F$ [28]. Therefore, we observe a spin current that has an oscillatory behavior with UL/v_F when this difference spins are equal to $\pi k_F L/4$. It can be seen that the conductance versus the incident chemical potentials in the superlattice has an oscillatory behavior, which can tune the spin current due to the exchange field of the FMG. Meanwhile, the up spin conductance ($G_\uparrow$) is reaches zero, whereas $G_\downarrow$ has maximum value of 0.7 at $U = 634$ (meV) as shown in Figure 2 (b). In the state, the conductance spectrum oscillates between 0.7 and zero. In this case, the electron conductance ($G_\uparrow + G_\downarrow$) is positive. Therefore, spin current in NG/FMG/NG superlattice junctions is irreversible. As shown in this figure, the up/down spin conductance reaches zero for some chemical potentials, which is controllable by the gate voltage. Therefore, the FMG superlattice can play as a spin filter that controls the spin current. We have observed that increasing the number of magnetic barriers, as $N = 100$, is the most efficient spin filter value. Namely, our scheme provides a spin filtering device through creating the superlattice of NG/FMG/NG. As a result, we can develop a spin filter in electronic devices.

As shown in Figure 3, there is a finite spin current that oscillates with respect to U without damping through the superlattice ($N = 100$). Therefore, by changing the gate voltage, we could reverse the spin-up and down current.

To assess the role of the well, barrier width, and Fermi energy in the spin current, Figure 4 (a) displays spin conductance G_s as a function of the chemical potential U for $N = 100$ and $D = 42.5$ (nm) for $L = 4.5$ (nm) and $L = 30$ (nm). Figure 4 shows a minimum/maximum of the spin current, describing the conductance's spin dependence for some chemical potentials. For spin conductance equal to zero, Figure 4 (a) reveals that the minimum/maximum value is the same minimum/maximum value of spin current shown in Figure 3. As L increases, the period value of spin conductance is reduced. Namely, the period of the conductance spectrum was broken. This behavior may be due to $U \gg E_F$ isn't satisfied for small L. Meanwhile, by increasing $k_F LU/E_F$ for large L, we can again illustrate periodic behavior in the conductance spectrum with respect to U.

Furthermore, the spin conductance versus incident the chemical potential for $E_F = 300$ (meV) and $E_F = 250$ (meV) are illustrated in Figure 4 (b). Clearly, the minimum/maximum value of spin-up and down is shifted, which means the spin current is reversed. It results from the spin-up and down that can be reversed by changing E_F. Figure 4 (c) shows the spin-dependence of conductance as a function of U for barrier width $D = 42.5$ (nm) and $D = 60$ (nm). Similar to Figure 4 (b), spin-up and down are shifted, so, the spin current is reversed. Overall, we found that we could reverse the spin current by tuning the parameters such as Fermi energy, well, and barrier width, presented in Figure 4.

To better understand the details of the well and barrier

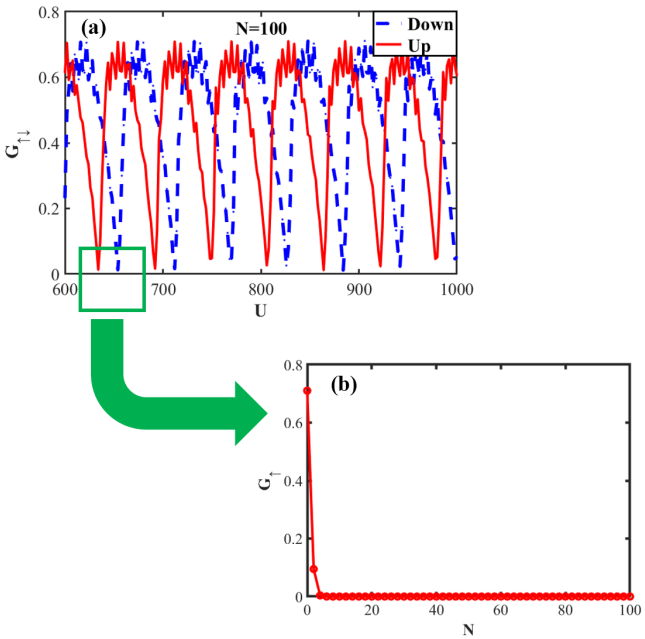

Figure 2. Spin-resolved as a function of the chemical potential U for magnetic barriers with $N = 100$ in FMG superlattice (solid red is spin-up and dashed blue is spin-down). (b) The conductance of spin-up as a function of the N at $U = 634$ (meV).

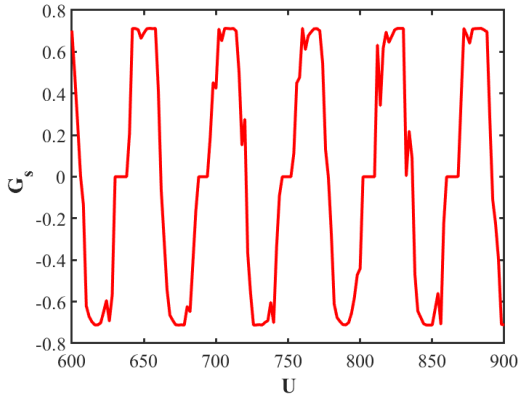

Figure 3. Spin conductance as a function of the chemical potential U for $D = 42$ (nm), $L = 4.5$ (nm), and $N = 100$.

widths in the spin current, we calculated the spin conductance as a function of the well and barrier widths, which are illustrated in Figure 5. Note that in Figure 5 (a), barrier width is $D = 60$ (nm) and $N = 100$. As illustrated in Figure 5 (a), the conductance spectrum has an oscillatory behavior due to quantum interference of radiant and electron's reflection through the normal graphene. Furthermore, the spin conductance as a function of the barrier width with parameters such as $N = 100$, $h = 10$ (meV), $E_F = 300$ (meV), $U = 800$ (meV), and $L = 4.5$ (nm), are shown in Figure 5 (b). We noticed that the conductance plot, similar to Figure 5 (a), has an oscillatory behavior, and the spin conductance strongly depends on the barrier width. Also, we observed that by increasing D, the conductance is neither reduced nor destroyed. Accordingly, we know from the Schrodinger wave equation's definition that the conductance should be destroyed by increasing the barrier height. In contrast, our results revealed that the conductance was not changing by increasing barrier width D. This result is in contrast with the prediction of Schrodinger's equation of wave functions in the different layers of MTJ [44].

Figure 6 exhibits the spin conductance in terms of the exchange field for different wells, barrier widths, and chemical energy. As can be seen, the conductance shows a modulating behavior. This quantum modulating behavior is due to the making of the two components of the spin conductance, which are calculated based on a two-dimensional massless Dirac equation for graphene [44]. The transport of spin-up and down electrons can produce the conductance of the junction. Also, modulating behavior exhibits that the gate

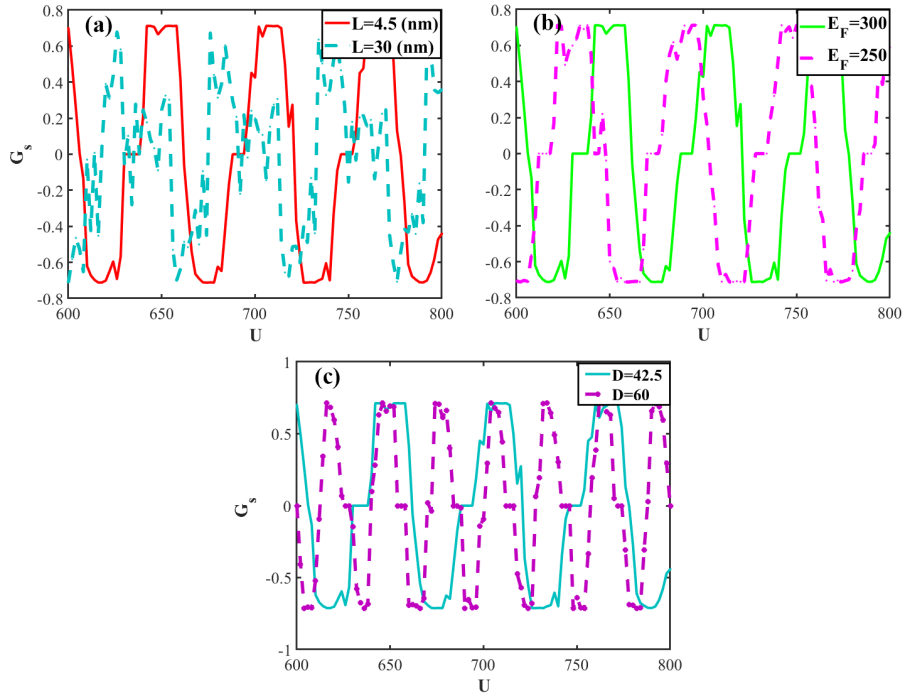

Figure 4. Spin conductance on the incident chemical potential for different; (a) well width, (b) Fermi energy and (c) barrier width. (a) The spin conductance for $L = 4.5$ (nm) (red line) and $L = 30$ (nm) (blue line). (b) Green and pink lines display the spin conductance for $E_F = 300$ (meV) and $E_F = 250$ (meV) respectively. (c) The spin conductance is for $D = 42.5$ (nm) (purple line) and $D = 60$ (nm) (blue line).

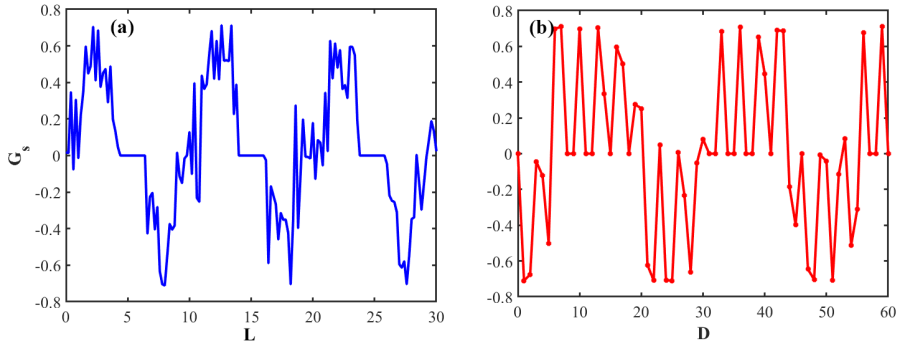

Figure 5. Spin conductance as a function of the (a) well width (L) and (b) barrier width (D).

voltage can control the exchange field. As L increases, the conductance spectrum is slightly reduced to that presented in Figure 6 (a). Also, in Figure 6 (b), the spin conductance shifts due to an increase in U. In other words, the minimum/maximum value of spin-up and down is changing. Namely, by tuning the chemical energy, we can reverse the spin current. As a result, we can control the spin current. By the result in Figure 6 (c), we can understand better and assess the barrier width role. We saw that the sharpness of peaks is reduced in the case of $D = 60$ (nm), but the conductance spectrum has maintained its periodic order. Mainly, the conductance spectrum is still able to control spin current. The oscillation reduction may be due to a decrease and/or elimination of the random spin motions.

4. Conclusion

We calculated the spin transport of normal/ferromagnetic/normal graphene superlattices where the ferromagnetic graphene is connected with a gate electrode. The spin current reveals an oscillatory behavior with the chemical potential due to the exchange field in the ferromagnetic graphene. Therefore, the spin current is controllable by the tune gate electrode. By tuning the gate voltage, we can control the spin-up/down currents. As a result, it is possible to generate the up/down spins filtering. Furthermore, the conductance spectrum is shifted. Particularly, the spin current is reversed as we increase the barrier width (D) and Fermi energy (E_F). In the case of chemical energy, the conductance observes modulating behavior, which indicates that the exchange field can be tuned by the gate voltage, too. Moreover, we found that the conductance is reduced

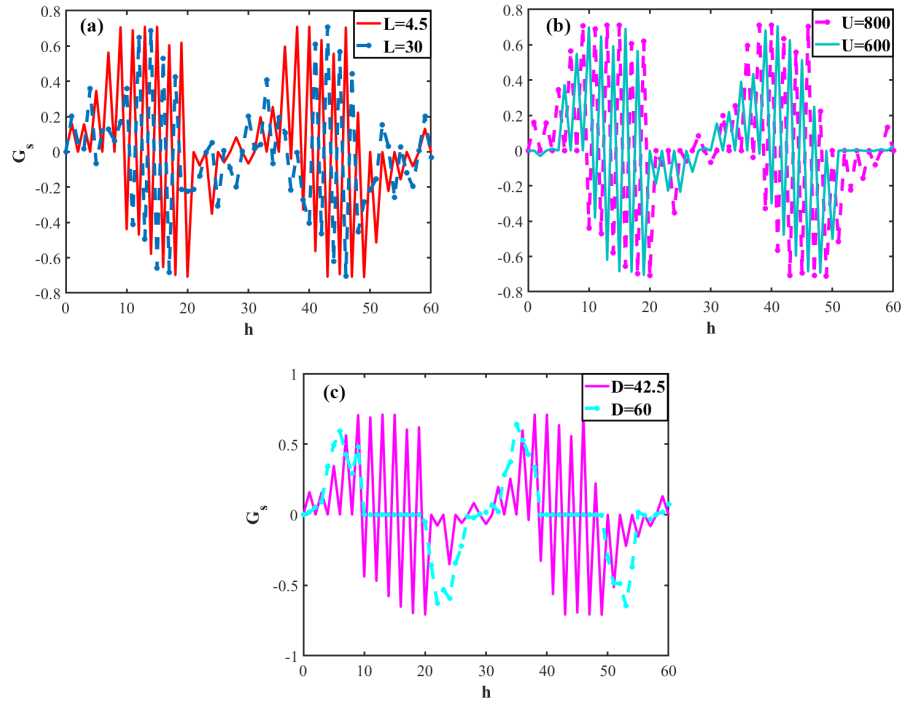

Figure 6. Spin conductance on the exchange field for different; (a) well width, (b) chemical energy, and (c) barrier width. (a) The spin conductance for $L = 4.5$ (nm) (red line) and $L = 30$ (nm) (blue line). (b) Green and pink lines display the spin conductance for $U = 800$ (meV) and $U = 600$ (meV), respectively. (c) The spin conductance for $D = 42.5$ (nm) (pink line) and $D = 60$ (nm) (blue line).

by increasing the barrier width. Understanding the spin conductance of the ferromagnetic graphene superlattices may have significant applications for making devices based on graphene superlattices.

Acknowledgment
We would like to thank Shahid Rajaee Teacher Training University for supporting this work.

Authors Contributions
Authors have contributed equally in preparing and writing the manuscript.

Availability of Data and Materials
The data that support the findings of this study are available from the corresponding author upon reasonable request.

Conflict of Interests
The authors declare that they have no known competing financial interests or personal relationships that could have appeared to influence the work reported in this paper.

References

[1] Y. Cao, D. Rodan-Legrain, O. Rubies-Bigorda, J. M. Park, K. Watanabe, T. Taniguchi, and P. Jarillo-Herrero. "Tunable correlated states and spin-polarized phases in twisted bilayer-bilayer graphene.". *Nature*, **583**:215–20, 2020.

[2] A. Avsar, H. Ochoa, F. Guinea, B. Özyilmaz, B. J. van Wees, and I. J. Vera-Marun. "Colloquium: Spintronics in graphene and other two-dimensional materials.". *Rev. Mod. Phys.*, **92**:021003, 2020. DOI: https://doi.org/10.1103/RevModPhys.92.021003.

[3] A. David, P. Rakyta, A. Kormányos, and G. Burkard. "Induced spin-orbit coupling in twisted graphene-transition metal dichalcogenide heterobilayers: Twistronics meets spintronics.". *Phys. Rev. B*, **100**:085412, 2019. DOI: https://doi.org/10.1103/PhysRevB.100.085412.

[4] J. S. Friedman, A. Girdhar, R. M. Gelfand, G. Memik, H. Mohseni, A. Taflove, B. W. Wessels, J. P. Leburton, and A. V. Sahakian. "Cascaded spintronic logic with low-dimensional carbon.". *Nat. Commun.*, **8**:15635, 2017. DOI: https://doi.org/10.1038/ncomms15635.

[5] H. Naganuma, V. Zatko, M. Galbiati, F. Godel, A. Sander, et al. "A perpendicular graphene/-ferromagnet electrode for spintronics.". *Appl. Phys. Lett.*, **116**:173101, 2020. DOI: https://doi.org/10.1063/1.5143567.

[6] B. Pathak I. Choudhuri, P. Bhauriyal. "Recent advances in graphene-like 2D materials for spintronics applications.". *Chem. Mater.*, **31**:8260–85, 2019. DOI: https://doi.org/10.1021/acs.chemmater.9b02243.

[7] J. Sichau, M. Prada, T. Anlauf, T. J. Lyon, B. Bosnjak, L. Tiemann, and R. H. Blick. "Resonance microwave measurements of an intrinsic spin-orbit coupling gap in graphene: A possible indication of a topological state. ". *Appl. Phys. Lett.*, **122**:046403, 2019. DOI: https://doi.org/10.1103/PhysRevLett.122.046403.

[8] Y. Zheng and T. Ando. "Hall conductivity of a two-dimensional graphite system.". *Phys. Rev. B*, **65**:245420, 2002. DOI: https://doi.org/10.1103/PhysRevB.65.245420.

[9] V. P. Gusynin and S. G. Sharapov. "Unconventional integer quantum Hall effect in graphene.". *hys. Rev. Lett.*, **95**:146801, 2005. DOI: https://doi.org/10.1103/PhysRevLett.95.146801.

[10] Q. Sun, X. Yao, O. Groning, K. Eimre, C. A. Pignedoli, K. Mullen, A. Narita, R. Fase, and P. Ruffieux. "Coupled spin states in armchair graphene nanoribbons with asymmetric Zigzag edge extensions.". *Nano Lett.*, **20**:6429–36, 2020. DOI: https://doi.org/10.1021/acs.nanolett.0c02077.

[11] J. Kang, O. Vafek, and Symmetry. "Maximally localized wannier states, and a low-energy model for twisted bilayer graphene narrow bands.". *Phys. Rev. X*, **8**:031088, 2018. DOI: https://doi.org/10.1103/PhysRevX.8.031088.

[12] K. S. Novoselov, A. K. Geim, S. V. Morozov, D. Jiang, Y. Zhang, S. V. Dubonos, I. V. Grigorieva, and A. A. Firsov. "Electric field effect in atomically thin carbon films.". *Science*, **306**:666, 2004. DOI: https://doi.org/10.1126/science.1102896.

[13] N. Abedpour, A. Esmailpour, R. Asgari, and M. Reza Rahimi Tabar. "Conductance of a disordered graphene superlattice.". *Phys. Rev. B*, **79**:165412, 2009. DOI: https://doi.org/10.1103/PhysRevB.79.165412.

[14] A. Esmailpour, F. Pakdel, and R. Jahanaray. "Effect of gap fluctuations on conductance of monolayer and bilayer graphene superlattices.". *Phys. E: Low-dimens. Syst. Nanostruct.*, **54**:214–9, 2013. DOI: https://doi.org/10.1016/j.physe.2013.06.023.

[15] J. J. Wang, D. Rodan-Legrain, L. Bretheau, D. L. Campbell, B. Kannan, and D. Kim. "Coherent control of a hybrid superconducting circuit made with graphene-based van der Waals heterostructures.". *Nat. Nanotechnol.*, **14**:120–5, 2019.

[16] H. S. Arora, R. Polski, Y. Zhang, A. Thomson, et al. "Superconductivity in metallic twisted bilayer graphene stabilized by WSe_2. ". *Nature*, **583**:379–84, 2020. DOI: https://doi.org/10.1038/s41586-020-2473-8.

[17] Y. Saito, J. Ge, K. Watanabe, T. Taniguchi, and A. F. Young. "Independent superconductors and correlated insulators in twisted bilayer graphene.". *Nat. Phys.*, **16**:926–30, 2020.

[18] J. Li, H.-B. Leng, H. Fu, K. Watanabe, T. Taniguchi, X. Liu, C. X. Liu, and J. Zhu. "Superconducting proximity effect in a transparent van der Waals superconductor-metal junction.". *Phys. Rev. B*, **101**:195405, 2020. DOI: https://doi.org/10.1103/PhysRevB.101.195405.

[19] F. Jedema, A. Filip, and B. van Wees. "Electrical spin injection and accumulation at room temperature in an all-metal mesoscopic spin valve.". *Nature*, **410**:34–38, 2001.

[20] X. Lou, C. Adelmann, S. A. Crooker, E. S. Garlid, J. Zhang, K. S. Madhukar Reddy, S. D. Flexner, C. J. Palmstrøm, and P. A. Crowel. "Electrical detection of spin transport in lateral ferromagnet-semiconductor devices.". *Nat. Phys.*, **3**:197–202, 2007.

[21] N. Tombros, C. Jozsa, M. Popinciuc, H. T. Jonkman, and B. J. van Wees. "Electronic spin transport and spin precession in single graphene layers at room temperature.". *Nature*, **448**:571–4, 2007.

[22] J. S. Moodera, L. R. Kinder, T. M. Wong, and R. Merservey. "Large magnetoresistance at room temperature in ferromagnetic thin film tunnel junctions.". *Phys. Rev. Lett.*, **74**:3272, 1995.

[23] S. Yuasa, T. Nagahama, and Y. Suzuki. "Spin-polarized resonant tunneling in magnetic tunnel junctions. ". *Science*, **297**:234, 2002. DOI: https://doi.org/10.1126/science.1071300.

[24] H. F. Mu, Z. G. Zhu, Q. R. Zheng, B. Jin, Z. C. Wang, and G. Su. "Theoretical consideration of spin-polarized resonant tunneling in magnetic tunnel junctions.". *Phys. Lett. A*, **323**:298, 2004. DOI: https://doi.org/10.1016/j.physleta.2004.01.076.

[25] J. Yang, J. Wang, Z. M. Zheng, D. Y. Xing, and C. R. Chang. "Quantum oscillations of tunneling magnetoresistance in magnetic tunnel junctions. ". *Phys. Rev. B*, **71**:214434, 2005. DOI: https://doi.org/10.1103/PhysRevB.71.214434.

[26] J. D. Lu. "The effect of the bias on the electron transport properties in a magnetic double-barrier nanostructure.". *Sol. Stat. Commun.*, **147**:242, 2008. DOI: https://doi.org/10.1016/j.ssc.2008.06.012.

[27] H. Haugen, D. Huertas-Hernando, and A. Brataas. "Spin transport in proximity-induced ferromagnetic graphene. ". *Phys. Rev. B*, **77**:115406, 2008.

[28] T. Yokoyama. "Controllable spin transport in ferromagnetic graphene junctions.". *Phys. Rev. B*, **77**:073413, 2008. DOI: https://doi.org/10.1103/PhysRevB.77.073413.

[29] C. Bai and X. Zhang. "Large oscillating tunnel magnetoresistance in ferromagnetic graphene single tunnel junction.". *Phys. Lett. A*, **372**:725, 2008. DOI: https://doi.org/10.1016/j.physleta.2007.08.050.

[30] A. L. Friedman, O. M. J. vant Erve, C. H. Li, J. T. Robinson, and B. T. Jonker. "Homoepitaxial tunnel barriers with functionalized graphene-on-graphene for charge and spin transport.". *Nat. Commun.*, **5**:3161, 2014. DOI: https://doi.org/10.1038/ncomms4161.

[31] C. S. Huang, Y. Yang, Y. C. Tao, and J. Wang. "Identifying the graphene d-wave superconducting symmetry by an anomalous splitting zero-bias conductance peak.". *New J. Phys.*, **22**:033018, 2020. DOI: https://doi.org/10.1088/1367-2630/ab74a6.

[32] M. D. Ashama and A. H. Phillips. "Coherent spin transport properties of ferromagnetic graphene superlattice unit cell.". *Phys. E: Low-dimens. Syst. Nanostruct.*, **113**:97–102, 2019. DOI: https://doi.org/10.1016/j.physe.2019.05.003.

[33] J. C. Meyer, A. K. Geim, M. I. Katsnelson, K. S. Novoselov, T. J. Booth, and S. Roth. "The structure of suspended graphene sheets.". *Nature*, **446**:60–63, 2007.

[34] K. Pi, W. Han, K. M. McCreary, Y. Li, Jared J. I. Wong, A. G. Swartz, and R. K. Kawakami. "Tunneling spin injection into single layer graphene.". *Phys. Rev. Lett.*, **105**:167202, 2010.

[35] Z. Zhao, X. Zhai, and G. Jin. " Thermally driven spin transport through a transverse-biased zigzag-edge graphene nanoribbon.". *J. Phys.: Condens. Matter.*, **24**:095302–5, 2012.

[36] A. Esmailpour, H. Meshkin, and M. Saadat. "Conductance of disordered strain-induced graphene superlattices.". *Phys. E: Low-dimens. Syst. Nanostruct.*, **50**:57–60, 2013. DOI: https://doi.org/10.1016/j.physe.2013.02.014.

[37] M. Esmailpour, A. Esmailpour, R. Asgari, M. Elahi, and M. R. Rahimi Tabar. "Effect of a gap opening on the conductance of graphene superlattices.". *Sol. Stat. Commun.*, **150**:655–9, 2010. DOI: https://doi.org/10.1016/j.ssc.2009.12.024.

[38] A. Esmailpour, H. Meshkin, and R. Asgari. "Conductance of graphene superlattices with correlated disorder in velocity profiles.". *Sol. Stat. Commun.*, **152**:1896–901, 2012. DOI: https://doi.org/10.1016/j.ssc.2012.06.021.

[39] A. Esmailpour, M. Abdolmaleki, and M. Saadat. "Dc conductance of ordered and disordered silicene superlattices. ". *Phys. E: Low-dimens. Syst. Nanostruct.*, **77**:144–8, 2016. DOI: https://doi.org/10.1016/j.physe.2015.11.006.

[40] Z. P. Niu, F. X. Li, B. G. Wang, L. Sheng, and D. Y. Xing. "Spin transport in magnetic graphene superlattices.". *Eur. Phys. J. B*, **66**:245–250, 2008. DOI: https://doi.org/10.1140/epjb/e2008-00413-5.

[41] Í. S. F. Bezerra and Jonas R. F. Lima. "Transport properties of magnetic graphene superlattices with modulated Fermi velocity.". *Solid State Communications*, **340**:114511, 2021. DOI: https://doi.org/10.1016/j.ssc.2021.114511.

[42] J. R. F. Lima, L. F. C. Pereira, and C. G. Bezerra. "Controlling resonant tunneling in graphene via Fermi velocity engineering.". *J. Appl. Phys.*, **119**:244301, 2016. DOI: https://doi.org/10.1063/1.4953865.

[43] S. Datta. "Electronic transport in mesoscopic systems.". *Cambridge University Press*, , 1995. DOI: https://doi.org/10.1017/CBO9780511805776.

[44] B. Soodchomshom, I. M. Tang, and R. Hoonsawat. "Quantum modulation effect in a graphene-based magnetic tunnel junction.". *Phys. Lett. A*, **372**:5054–8, 2008. DOI: https://doi.org/10.1016/j.physleta.2008.05.051.